Sakarya Üniversitesi Fen Bilimleri Dergisi
Sakarya University Journal of Science

e-ISSN : 2147-835X
Publisher : Sakarya University

Vol. 29, No. 5, 602-625, 2025
DOI: https://doi.org/10.16984/saufenbilder.1735274

Review Article

Lead-Free Alternatives for Radiation Shielding in Medical Environments: A Comprehensive Review

Khalid Hani Abushahla[1*], Halil Arslan[2]

[1] Biomedical Technologies Application and Research Center (Biyotam), Sakarya University of Applied Sciences, Sakarya, Türkiye, 22500305002@subu.edu.tr, ror.org/01shwhq58
[2] Electrical and Electronics Engineering Department, Sakarya University of Applied Sciences, Sakarya, Türkiye, harslan@subu.edu.tr, ror.org/01shwhq58
[*]Corresponding Author

ARTICLE INFO

Keywords:
Lead-free materials
Radiation
Shielding
Medical radiology

Article History:
Received: 05.07.2025
Revised: 13.08.2025
Accepted: 29.08.2025
Online Available: 21.10.2025

ABSTRACT

In radiography, effective radiation shielding plays a vital role in safeguarding patients, medical staff, and the public, as well as in preserving the integrity of surrounding materials. Traditionally, lead has been the primary shielding material due to its high atomic number and density, which provide efficient attenuation of radiation. However, lead presents several challenges, including significant weight, toxicity, long-term health risks, and serious environmental concerns. Lead waste is classified as hazardous due to its non-biodegradable nature, its potential for contaminating soil and water, and the difficulties associated with safe disposal and recycling processes. These issues have driven the search for safer and more sustainable alternatives. Recent advancements have led to the development of lead-free shielding materials designed to replace conventional lead-based shields. Among these, lead-free multilayered polymer composites have emerged as promising substitutes, often enhanced with elements such as bismuth, tungsten, barium, tin, cadmium, gadolinium, antimony, and molybdenum to improve their radiation protection capabilities. This study examines the potential of these alternatives to address the limitations of traditional lead shielding, with a particular focus on their development and application in medical settings. By reducing toxicity, lowering weight, and improving recyclability, these materials offer a more environmentally friendly and health-conscious approach to radiation protection.

1. Introduction

1.1. Types and biological effects of ionizing and non-ionizing radiation

Radiation is the process through which energy travels or propagates in the form of waves or particles through space or through some other medium [1]. Radiation is classified into ionizing radiation (IR) and non-ionizing radiation (NIR). IR, such as high-energy photons, neutrons, protons, and alpha particles, has sufficient energy to liberate tightly bound electrons from atoms, creating charged particles (ions). This ionization process can damage biological tissues and lead to severe health effects, including acute radiation syndrome, organ damage, and an increased risk of cancers such as leukemia. In contrast, NIR (e.g., visible light, infrared, and radio waves) has lower energy and cannot ionize atoms or molecules [2-4].

Among ionizing radiation are alpha particles, consisting of two protons and two neutrons (helium nuclei), making them relatively heavy and positively charged. Due to their high mass and charge, alpha particles have low penetration power and can be stopped by a sheet of paper or the outer layer of human skin [5, 6].

Other types of ionizing radiation are beta particles, which are high-speed electrons or

Cite as: K. H. Abushahla, H. Arslan, "Lead-free alternatives for radiation shielding in medical environments: A comprehensive review," Sakarya University Journal of Science, vol. 29, no. 5, pp. 602-625, 2025. https://doi.org/10.16984/saufenbilder.1735274

positrons with moderate penetration power. They are more penetrating than alpha particles but can be stopped by materials such as plastic, glass, or a few millimeters of aluminum [7].

Moreover, X-rays and gamma rays are electromagnetic radiation with very high energy and penetration power [8]. In recent years, their use in medicine has expanded with the development of new technologies and applications in diagnostics, especially in imaging and in some therapy protocols [9-11].

Radiation is a crucial component in modern medicine, encompassing electromagnetic waves and particulate radiation. Advanced imaging techniques have improved diagnostic and therapeutic procedures. X-ray systems create images of internal structures, while CT provides detailed cross-sectional views. Positron emission tomography (PET) evaluates physiological and metabolic processes. Other radiation-based methods include radionuclide imaging for organ function assessment, laser technology for precise surgical interventions, and ultraviolet radiation for therapeutic purposes. Radiation processing is also used in industrial contexts for material properties enhancement and sterilization [12].

1.2. Applications of radiation in medicine and industry

Radiation is widely applied in medicine and industry, but its use requires careful control due to potential health hazards. It is essential in medical imaging, cancer therapy, industrial inspection, material processing, and research. Radiation injury severity can be affected by a wide range of confounding factors, including age, gender, prior medical conditions, radiation types, duration, and dose rates. Radiation types, radiation dosages, and radiation dose rates are positively linked with the death rate [13].

1.3. Radiation hazards and protective measures

Although radiation has many uses in industry and medicine, there are serious hazards associated with it, particularly when exposure is extended. Ionizing radiation penetrates biological tissues, damages DNA, produces free radicals, and interferes with cellular processes. This may result in health problems such as an elevated risk of cancer due to genetic mutations, severe burns from radiation, and possible genetic harm from the ionizing effects of X-rays and gamma rays. Acute Radiation Syndrome, which is marked by nausea, vomiting, and death, can also be brought on by high exposure. The most serious long-term health dangers in the medical field are from the ionizing effects of X-rays and gamma rays, even while other forms of radiation cause sunburn and heating of tissues [14].

To reduce the risks of radiation exposure, various protective measures are implemented. In medical imaging, especially in radiation-based procedures, three fundamental principles—time, distance, and shielding—are crucial for minimizing exposure. Decreasing exposure time and increasing distance are both effective strategies, as radiation exposure is inversely proportional to the square of the distance from the source [15, 16]. Shielding plays a crucial role in protecting healthcare professionals. Shielding devices such as lead aprons, glasses, and thyroid protectors are designed to absorb and block radiation, thus significantly reducing exposure [17].

Despite their cost and potential discomfort, these devices are vital for ensuring safety. Shielding is universally important across all forms of medical imaging, as it provides an additional layer of protection beyond merely managing exposure time and distance. By effectively utilizing shielding, healthcare professionals can substantially decrease their radiation dose, making it a critical component of radiation safety practices [18].

1.4. ALARA principle and shielding material selection

The ALARA principle was generally introduced by the ICRP in 1977 under the general term of “As Low as Reasonably Achievable” [19], and then introduced in endourology by Greene et al. in 2011 [20]. In medical imaging, the ALARA principle is crucial for minimizing radiation exposure while maintaining the required diagnostic quality. Based on this idea, the lowest possible effective radiation dose is used during radiological procedures [21]. For radiation shielding materials to be both practical and effective, a number of important criteria must be balanced.

Due to their increased likelihood of interacting with radiation and resulting in increased energy transfer, high atomic number (high-Z) materials with high-density materials such as bismuth (Bi), lead (Pb), and barium (Ba) are favored [22]. However, if employed in greater thicknesses, materials with lower atomic numbers and densities can also offer efficient shielding, producing comparable protective effects to those of high-Z materials. Aside from the type and intensity of radiation, other important factors to consider are the handling, weight, and cost of the materials. In addition to efficiently attenuating or absorbing radiation, effective shielding materials should also be affordable and manageable in real-world applications. Traditional materials are effective, but they frequently have drawbacks like high cost, heaviness, and toxicity. This situation has led to continuous research to create better substitutes [23].

1.5. Role and limitations of lead

Lead (Pb) is widely recognized as the most toxic heavy metal in radiation shielding contexts, and, along with mercury (Hg), arsenic (As), cadmium (Cd), and chromium (Cr), it ranks among the top priority metals of public health concern due to their ability to cause systemic toxicity, multi-organ damage, and carcinogenic effects even at low exposure levels [24, 25]. Due to its high atomic number (Z) and favorable interaction cross-section, which make it extremely effective at blocking photon radiation, lead has long been utilized as a radiation shield [26]. Lead can be found in various forms, including lead bricks, leaded glass, leaded plastics, and lead shot, to suit different applications [27]. Its density and compactness improve its shielding ability, which makes it very suitable for space-limited applications, like nuclear medicine and medical radiology [28, 29]. For example, clinical personnel also use lead-based protective materials when performing radiological imaging, like X-ray image-guided interventional radiology procedures. Furthermore, from an economic standpoint, there is no commercial product with a similarly excellent shielding capacity and workability as lead [30]. However, lead has significant drawbacks, including its toxicity and high cost, which restrict its use in many applications. Lead-based materials pose serious health risks due to their toxicity and the potential formation of harmful particles on surfaces, which contributes to lead's decreased desirability despite its effective shielding properties [31].

1.6. Lead-free alternatives

Furthermore, lead aprons, which are frequently used in medical settings, are traditionally very heavy and can be uncomfortable and problematic for the back when worn for extended periods [32]. These issues highlight the need for safer, non-toxic, and more sustainable alternatives for radiation shielding, as lead has poor strength and hardness also limit its durability [29]. Due to the disadvantages of lead, scientists are investigating alternative materials for radiation shielding. Various lead-free materials have been explored and categorized into glasses, ceramics, pure metals, polymers, concrete, and various composites. Among these materials, the literature often highlights metals and metals under different compositions and variations as key elements, with the most common ones being Bismuth [33-36], Tungsten [37, 38], Barium [39], Tin [40], Molybdenum [41], Cadmium [42], Gadolinium [43] and Antimony [44].

These substitutes for lead are meant to limit the negative impacts on patients, medical personnel, and the environment while encouraging safer and more environmentally friendly procedures. This review examines radiation-shielding materials, which contain Bismuth, Tungsten, Barium, Tin, Molybdenum, Cadmium, Gadolinium, and Antimony. Each of these materials has the potential to replace lead in radiation shielding, with an emphasis on their characteristics, efficacy, and possible uses in healthcare environments. In other words, alternatives are discussed in this review, going over their makeup, radiation-attenuation properties, and potential applications in medical radiation protection. Research is still ongoing to optimize these materials for particular uses, weighing the advantages against any potential disadvantages.

2. Lead-Free Alternative Materials

2.1. Material selection criteria

The essential characteristics of some materials that improve the radiation-shielding efficacy are listed in Table 1, together with those of lead. Lead is widely used as a reference material due to its established shielding properties. The other materials are typically incorporated as additives in various chemical compositions, some of which are discussed in detail in the following sections (see Table 1).

2.2. Physical properties of elements

Basic properties, including atomic number, weight, density, and melting point, of the elements of interest and lead are given in Table 1. Bismuth (Bi), a non-toxic, high-density heavy metal, is increasingly valued for its strong radiation absorption properties, making it a promising lead-free alternative for shielding applications. Its oxide form, Bi_2O_3, offers enhanced durability and efficiency in blocking radiation, competing with lead-based materials while addressing health and environmental concerns. Tungsten (W) also stands out as an effective shielding material due to its high atomic number and density, offering good protection against radiation. Its thermal stability and resistance to environmental degradation make it ideal for high-temperature applications, even though there are still issues with its processing.

Barium (Ba), particularly in oxide form (BaO), enhances gamma radiation attenuation in glass systems and other composites, contributing to the development of sustainable, lead-free shielding solutions.

Other metals, such as tin (Sn), cadmium (Cd), gadolinium (Gd), antimony (Sb), and molybdenum (Mo), also offer valuable contributions to radiation shielding technologies. Their unique properties, including high atomic numbers and densities, help improve material performance across diverse applications. These metals pave the way for advanced, eco-friendly shielding materials that meet the growing need for non-toxic, safer alternatives.

Table 1. Basic properties of lead and its radiation-shielding alternatives

Element	Latin Names	Symbol	Atomic Number	Atomic Weight	Density (g/cm³)	Melting Point (°C)
Lead	Plumbum	Pb	82	207.2	11.3	327.5
Bismuth	Bismuthum	Bi	83	209	9.78	271.3
Tungsten	Wolframium	W	74	183.9	19.3	3410
Barium	Barium	Ba	56	137.3	3.62	727
Tin	Stannum	Sn	50	118.7	7.31	231.9
Cadmium	Cadmium	Cd	48	112.41	8.65	321
Gadolinium	Gadolinium	Gd	64	157.25	7.9	1312
Antimony	Stibium	Sb	51	121.76	6.68	630.6
Molybdenum	Molybdaenum	Mo	42	95.95	10.28	2623

3. Detailed Material Analysis

3.1. Bismuth (Bi)

Bismuth (Bi) is a non-toxic, inexpensive heavy metal with distinctive properties, including high specific gravity, photoluminescence, photoelectric and photovoltaic effects, strong oxidation ability, and water insolubility. It also has a white crystalline structure, high electrical resistance, and strong diamagnetic properties. The surface of Bi crystals typically displays iridescent rainbow colors due to interference effects from the oxide layer [45, 46].

Bismuth is known as the wonder metal due to its diverse oxidation states and strong tendency to form bismuth clusters as a result of the electrons' easy involvement in chemical combinations in the p orbital [47].

Bismuth, a metallic element with an atomic number of 83 and a mass number of 208.980, exhibits strong absorption characteristics for ionizing radiation due to its high atomic number. With a density of 9.78 g/cm³, melting point approximately 271.5°C, bismuth atoms contribute to increasing the material's overall density. The high concentration of electrons in bismuth enhances interactions between incident photons and the material's electrons, leading to a significant reduction in radiation intensity. This combination of high atomic number and density makes bismuth an excellent candidate for radiation protection and shielding, positioning it as a promising material for developing advanced shielding solutions in various applications.
Bismuth metal (99.5%) costs about $250/kg [48, 49].

Bismuth oxide is a highly effective lead alternative for radiation shielding. Its non-toxic nature, high atomic number, and 8.9 g/cm³ density. Its higher melting point compared to lead ensures better durability. As the bismuth oxide content increases, shielding parameters such as the half-value layer and tenth-value layer improve, enhancing its efficiency in blocking radiation. While lead is inexpensive and readily available due to its abundant supply and established mining processes, bismuth requires a larger initial investment. However, the long-term savings with bismuth come from reduced health and environmental protection needs [50-54].

Karimi et al. highlighted the growing demand for lead-free radiation shielding materials due to health concerns surrounding lead poisoning and leakage [55]. They compared various glass shields, including a commercial lead-based shield, four previously studied shields, and three new lead-free variants, by evaluating their shielding performance according to international standards (IEC 61331). The materials were analyzed for air kerma ratios, lead equivalent values, and shielding properties using Monte Carlo N-Particle eXtended (MCNPX) simulations [56].

Mass attenuation coefficients and effective atomic numbers (Zeff) were obtained from the XCOM database [57], covering the diagnostic X-ray energy range (40–120 keV). The study introduced three novel glasses—borate-based (Ir1), phosphate-based (Ir2), and silicate-based (Ir3). The Ir3 glass, composed of 0.05 Al_2O_3, 0.3 SiO_3, 0.1 BaO, and 0.55 Bi_2O_3 with a density of 5.4 g/cm³, along with the borosilicate-barium-based Tu glass, exhibited superior shielding properties, rivaling those of lead-based glass. These findings indicate that Ir3 and Tu glasses are promising alternatives as lead-free transparent shields for use in diagnostic X-ray energy ranges [55].

Yu et al. addressed the need for lightweight, lead-free X-ray shielding materials due to the toxicity and heaviness of conventional lead-based shields [58]. They synthesized bismuth titanate (BTO) particles and incorporated them into an epoxy resin (ER) matrix at varying loadings (0–65 wt%). The surface roughness and hardness of the BTO-ER composites were analyzed to assess their X-ray attenuation. Results showed that a 2 mm thick 65BTO-ER composite (0.65 $Bi_4Ti_3O_{12}$ + 0.35 CHO) achieved X-ray attenuation efficiencies of 97% at 80 kVp and 95% at 100 kVp, equivalent to 0.35 mm of lead but with half the weight. This demonstrates the potential of BTO-based composites as non-toxic, environmentally friendly alternatives to conventional lead shielding in diagnostic X-ray protection [58].

Khazaalah et al. focused on improving the efficiency of lead-free glass as a radiation shield while addressing the issues of dark brown bismuth glass and reducing waste glass accumulation in landfills by incorporating soda-lime-silica (SLS) glass waste [59].

Using the melt-quenching method, WBiBZn-SLS glass was fabricated at 1200 °C with varying concentrations of WO_3 (0–0.05 mol). The waste glass, composed of 74.1% SiO_2, provided the SiO_2 content. Radiation attenuation parameters were measured using narrow-beam geometry and X-ray fluorescence (XRF). Results indicated that increasing WO_3 concentration reduced the half-value layer and increased the linear attenuation coefficient (μ). WBiBZn-SLS glass, composed of WO_3 (0.05%), Bi_2O_3 (19%), ZnO (28.5%), and other components, proved to be a non-toxic, transparent, and effective radiation shielding material [59].

Li et al. tackled the challenge of designing flexible, lightweight radiation shielding materials for complex structures by developing for designing and assessing the safety of nuclear systems to predict γ-ray shielding performance [60, 61]. The study tested Pb- and Ta-doped Bi/PU coated fabric composites for shielding properties, mechanical performance, and wear resistance. The results showed that Ta doping enhanced γ-ray shielding, surpassing non-doped composites. However, Ta doping reduced wear resistance and tensile strength. The Bi/Ta/PU composite (50% Bi + 5% Ta + 45% $C_5H_6N_2O_2$) provides efficient, eco-friendly radiation protection, suitable for personal protective gear and collective shielding equipment, offering excellent γ-ray shielding while remaining lightweight and flexible [60].

Uosif et al. explored the need for effective, lead-free protective cover glass for solar cells in superstrate arrangements, where lightweight, radiation resistance, optical clarity, and structural integrity are essential [62]. Solar panels used in spacecraft suffer from reduced energy output due to UV and radiation damage to the cover glass. To address this, lead-free phosphate glasses with varying Bi_2O_3 content [xBi_2O_3–(40 − x)CaO–$60P_2O_5$, x = 5–30 mol%] were fabricated using high-temperature melting.

The study measured gamma shielding across multiple photon energies (81–2614 keV) and found that increasing Bi_2O_3 content enhanced the mass attenuation coefficient, though it decreased with rising photon energy. The $60P_2O_5$–$30Bi_2O_3$–10CaO glass exhibited the best overall performance, making it a promising lead-free option for radiation shielding in space-based solar cell applications [62].

Al-Hadeethi et al. investigated bismuth borate glass samples with varying compositions [(99-x) B_2O_3 + 1 Cr_2O_3 + (x) Bi_2O_3, where x = 0–25 wt%] using the melt quenching technique [63]. The mass attenuation coefficient (MAC) of the glasses was measured using four different point sources (^{241}Am, ^{133}Ba, ^{152}Eu, ^{137}Cs). The experimental MAC values closely matched theoretical results from XCOM [57], with deviations under 3%. The glass with 25 wt% Bi_2O_3 showed high attenuation, comparable to commercial lead borate glasses. Transmission factor (TF) values were found to be lower at lower energies and increased with photon energy. The addition of Bi_2O_3 reduced TF, enhancing shielding performance. Half-value layer (HVL) data highlighted greater photon penetration at higher energies, with HVL for BCrBi-20 glass being 0.171 cm at 0.0595 MeV and 4.334 cm at 1.408 MeV. The study also determined the fast neutron removable cross section (FNRC), showing that bismuth borate glasses, particularly the 25 wt% sample (74 B_2O_3 + CrO_3 + 25 Bi_2O_3), outperformed lead borate glass and concrete in radiation shielding [63].

Liu et al. explored the development of bismuth tungstate (Bi_2WO_6) nanostructures as potential alternatives to lead-based materials for radiation shielding [64].

With increasing nuclear activities and the need for low-toxicity protective materials, this study focused on fabricating Bi_2WO_6 nanosheets.
These nanosheets demonstrated gamma-ray attenuation properties comparable to lead-based materials for low-energy gamma rays. Given their lower toxicity, Bi_2WO_6 nanosheets are considered more suitable for fabricating personal protective equipment, offering promising prospects for shielding low-energy radiations and significant market potential in healthcare, nuclear facilities, aerospace, and other radiation-intensive industrial applications.[64].

Mass attenuation coefficient (MAC) values of the bismuth-based materials studied by the abovementioned groups are provided in Table 2 and Table 3 for various photon energies. These values were calculated for the composition of materials using the web database Epixs. Additionally, the MAC values are illustrated in Figure 1 as a function of energy, alongside those for lead.
As it can be seen from Table 2 ,3 and Figure 1, lead shows higher MAC values than bismuth-based materials at low photon energies (15–60 keV),

Table 2. Mass attenuation coefficients (cm^2/g) and lead equivalent for bismuth-based materials at various energies

Energy (MeV)	Karimi et al., 2020	Pb Eq.	Yu et al., 2021	Pb Eq.	Khazaalah et al., 2022	Pb Eq.	Li et al., 2023	Pb Eq.
0.015	64.9535	0.5844	57.2564	0.5151	43.0642	0.3874	65.0400	0.5851
0.02	47.5849	0.5528	42.9795	0.4993	26.2039	0.3044	48.0042	0.5577
0.03	16.7666	0.5526	15.1838	0.5004	9.0106	0.2970	16.9876	0.5599
0.04	9.7453	0.6791	7.2213	0.5032	4.2236	0.2943	8.0812	0.5631
0.05	5.4813	0.6844	4.0657	0.5076	2.3674	0.2956	4.5461	0.5676
0.06	3.4287	0.6886	2.5576	0.5137	1.4948	0.3002	2.8545	0.5733
0.08	1.6504	0.7006	1.2520	0.5315	0.7547	0.3204	1.6867	0.7160
0.1	3.0872	0.5563	2.7453	0.4947	1.2434	0.2241	3.1426	0.5663
0.15	1.1550	0.5733	1.0416	0.5171	0.5106	0.2535	1.1797	0.5856
0.2	0.5989	0.5986	0.5481	0.5478	0.2968	0.2967	0.6129	0.6127
0.3	0.2670	0.6624	0.2514	0.6237	0.1639	0.4067	0.2740	0.6799
0.4	0.1689	0.7283	0.1627	0.7013	0.1208	0.5208	0.1737	0.7487
0.5	0.1268	0.7866	0.1240	0.7696	0.1001	0.6213	0.1305	0.8095
0.6	0.1040	0.8344	0.1029	0.8255	0.0877	0.7036	0.1071	0.8592
0.8	0.0799	0.9043	0.0802	0.9071	0.0728	0.8237	0.0824	0.9320
1	0.0671	0.9486	0.0678	0.9587	0.0637	0.9000	0.0692	0.9780
1.5	0.0516	0.9925	0.0525	1.0090	0.0508	0.9760	0.0532	1.0228
2	0.0451	0.9826	0.0457	0.9950	0.0441	0.9599	0.0464	1.0096
3	0.0394	0.9341	0.0393	0.9317	0.0371	0.8788	0.0402	0.9512
4	0.0372	0.8883	0.0365	0.8723	0.0336	0.8026	0.0375	0.8964
5	0.0363	0.8521	0.0352	0.8252	0.0317	0.7423	0.0364	0.8528
6	0.0361	0.8241	0.0346	0.7887	0.0305	0.6956	0.0359	0.8190
8	0.0366	0.7845	0.0344	0.7373	0.0294	0.6299	0.0360	0.7713
10	0.0377	0.7583	0.0349	0.7032	0.0291	0.5865	0.0367	0.7397
15	0.0408	0.7214	0.0370	0.6554	0.0296	0.5245	0.0393	0.6955

Table 3. Mass attenuation coefficients (cm^2/g) and lead equivalent for bismuth-based materials at various energies

Energy (MeV)	Uosif et al., 2023	Pb Eq.	Al-Hadeethi et al., 2022	Pb Eq.	Liu et al., 2018	Pb Eq.
0.015	37.2820	0.3354	27.3167	0.2458	106.0480	0.9541
0.02	26.6959	0.3101	20.6541	0.2399	70.9025	0.8237
0.03	9.3782	0.3091	7.3601	0.2426	24.9387	0.8219
0.04	4.4689	0.3114	3.5480	0.2472	11.7914	0.8217
0.05	2.5345	0.3165	2.0346	0.2540	6.5854	0.8223
0.06	1.6130	0.3240	1.3097	0.2631	4.0985	0.8232
0.08	0.8167	0.3467	0.6794	0.2884	3.5603	1.5114
0.1	1.6674	0.3005	1.3995	0.2522	4.6158	0.8317
0.15	0.6635	0.3293	0.5696	0.2828	1.6824	0.8352
0.2	0.3701	0.3700	0.3257	0.3255	0.8439	0.8435
0.3	0.1901	0.4717	0.1744	0.4327	0.3494	0.8668
0.4	0.1337	0.5765	0.1260	0.5431	0.2068	0.8914
0.5	0.1078	0.6686	0.1032	0.6403	0.1473	0.9141
0.6	0.0928	0.7440	0.0897	0.7198	0.1163	0.9324
0.8	0.0755	0.8542	0.0739	0.8359	0.0849	0.9604
1	0.0654	0.9240	0.0644	0.9096	0.0692	0.9778
1.5	0.0517	0.9928	0.0511	0.9815	0.0518	0.9958
2	0.0448	0.9760	0.0441	0.9610	0.0456	0.9929
3	0.0378	0.8962	0.0367	0.8692	0.0412	0.9764
4	0.0344	0.8214	0.0328	0.7833	0.0402	0.9607
5	0.0325	0.7620	0.0305	0.7149	0.0404	0.9481
6	0.0314	0.7161	0.0290	0.6619	0.0411	0.9382
8	0.0304	0.6514	0.0274	0.5869	0.0432	0.9243
10	0.0302	0.6087	0.0267	0.5375	0.0454	0.9149
15	0.0310	0.5482	0.0265	0.4681	0.0510	0.9018

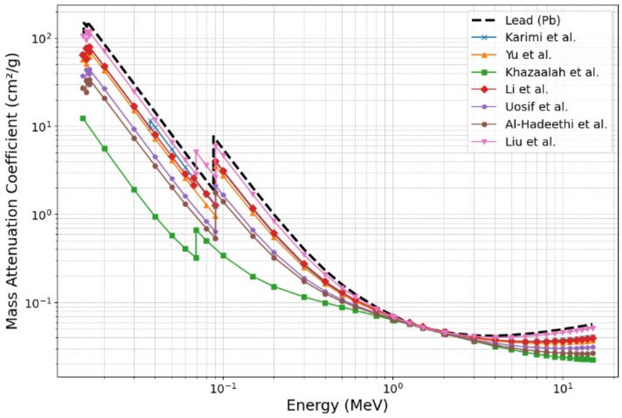

Figure 1. Mass attenuation coefficient values of various bismuth-based materials compared with lead

showing superior attenuation. For instance, at 15 keV, lead's MAC is 111.1520 cm²/g, while bismuth-based materials values range from 27.3167 cm²/g to 106.0480 cm²/g which indicates good performance although lead has the superiority. As the photon energy increases to moderate levels (100–1000 keV), bismuth's MAC values approach lead's values, as the performance of materials based on bismuth becomes comparable. For example, at 100 keV, lead's MAC is 5.5496 cm²/g, whereas bismuth-based materials values range from 1.2434 cm²/g to 4.6158 cm²/g also in the same interval when the energy is 800 keV MAC ranges between 0.0728 cm²/g (Khazaalah et al., 2022) and 0.0849 cm²/g (Liu et al., 2018) which almost equals the lead's MAC value 0.0884 cm²/g. At high energies (1000 keV and above), both materials exhibit significantly lower MAC values, with bismuth-based materials' values closely matching those of lead. At 1500 keV, lead's MAC is 0.0521 cm²/g, while bismuth's values range from 0.0511 cm²/g to 0.0532 cm²/g. Overall, while lead provides better attenuation at lower energies, bismuth-based materials offer comparable shielding effectiveness at moderate to high energies, making it a viable lead-free alternative for high-energy photon shielding applications.

3.2. Tungsten (W)

Tungsten (W), also known as wolfram, is a greyish-white to steel-grey metal characterized by extreme hardness, wear resistance, high melting point, high density, and excellent thermal and electrical conductivity; while pure tungsten is malleable and ductile, adding small amounts of carbon and oxygen enhances its hardness and brittleness [65]. Tungsten has an atomic weight of 183.9, an atomic number of 74, and a density of 19.3 g/cm³. It has a melting point of 3410°C and a boiling point of 5660°C, with a specific gravity of 19.3. Its crystalline form is gray-black and cubic, and it remains unoxidized in air at ordinary temperatures while being highly resistant to acids. Compared to lead (Pb), tungsten has a higher density with values of 19.3 g/cm³ [66, 67].

Tungsten's high melting point of 3387°C makes it a challenging material to machine or cast, but it has better shielding qualities than lead because of its high atomic number (Z). Due to its high melting point, tungsten is a high temperature material that has long been used to make light bulb filaments [68, 69]. Tungsten can be used to create radiation shielding materials with greater potential, lower costs, environmental friendliness, and improved optical properties when it is used in the development of such materials. Approximately, tungsten powder (99.999%) costs about $2900/kg [70].

Jamal AbuAlRoos et al. assessed tungsten carbide (WC), composed of 98.65% tungsten and 1.35% carbon, as a lead-free radiation shielding material for nuclear medicine [71]. The study analyzed WC using Field-Emission Scanning Electron Microscopy (FESEM) and energy dispersive X-ray (EDX), confirming its 99.9% purity and an average particle size of 40–50 µm. Discs of WC (0.1 cm, 0.5 cm, and 1.0 cm thickness) were compared to lead discs of similar thickness. Gamma spectroscopy with sources (^{123}I, ^{133}Ba, ^{152}Eu, and ^{137}Cs) across 0.160 MeV to 0.779 MeV energies measured attenuation properties. The experimental attenuation coefficients of WC and lead were compared to theoretical values from the NIST database. The results showed that gamma spectroscopy peaks exhibited a linear relationship with energy. Relative differences between measured and theoretical mass attenuation coefficients were within 0.19–5.11% for both materials. WC demonstrated lower half-value layers and mean free paths compared to lead, indicating its potential as an effective, lead-free alternative for radiation shielding in nuclear medicine [71].

Azman et al. reviewed tungsten carbide (WC), with a composition of 98.65% tungsten and 1.35% carbon, as a lead-free alternative for radiation shielding [72]. They addressed lead's drawbacks, including toxicity, weight, and opacity. Tungsten carbide's high atomic number, density, and excellent shielding properties make it a promising material. The review covers recent advancements in WC's physical properties, its application as a nanofilm for radiation shielding, and various deposition techniques for fabricating these films. It also discusses the morphological structure of WC nanofilms, as well as key challenges and future directions in this field [72].

Lee et al. proposed a dual-layered Pb-free shielding method to protect workers from external radiation exposure during the decommissioning of the Kori-1 nuclear power plant, which has been shut down since 2017 [73]. Using the Monte Carlo method, the study optimized and estimated the performance of various materials in terms of equivalent dose rate and radiation shielding effectiveness. The dual-layer Pb-free shielding outperformed conventional shields, with WC-Co showing particularly high performance in reducing external radiation during the dismantling of the steam generator (S/G). The simulation results provide valuable guidance for selecting materials and designing effective Pb-free dual-layer shields for this decommissioning process [73].

Das et al. examined metal-based polymer composites, specifically tungsten (W) – polymethyl methacrylate (PMMA), for radiation shielding [73]. They used FLUKA Monte Carlo [74] code to assess the effectiveness of W-PMMA composites in attenuating coupled neutron-gamma radiation. Results indicated that even a 20 vol% concentration of W particles significantly enhances the radiation shielding capability of PMMA. The study identified optimum heavy metal concentrations for shielding: 70 vol% W and 30 vol% Pb, with the Pb shield showing significantly higher doses. Additionally, the research explored double-layer laminates with W and PMMA in various configurations, finding that the new W-PMMA composite-based double-layer shield performed best in volumetric dose reduction, while single-layer W-PMMA composites offered the lowest specific dose [75]. Olivieri et al. developed lead-free x-ray shielding materials using Acrylonitrile-butadiene-styrene (ABS)-based composites with high tungsten and bismuth oxide content [75].

These composites, selected for their mechanical strength and ABS's availability as a recycled material, exhibited good filler dispersion within the polymer matrix while retaining their mechanical properties. The optimal formula, consisting of 70% WO_3 and 30% ABS, shows promise for lead-free x-ray shielding applications, including wearable personal protective equipment [76].

Mass attenuation coefficient (MAC) values of the tungsten-based materials studied by the abovementioned groups are provided in Table 4 for various photon energies. These values were calculated for the composition of materials using the web database Epixs. Additionally, the MAC values are illustrated in Figure 2 as a function of energy, alongside those for lead.

Considering the values given in Table 4 and plotted in Figure 2, some of the tungsten-based materials generally exhibit higher MAC values than lead at very low energies and in some low to moderate photon energies.

For example, at 15 keV, tungsten's MAC ranges from 77.2264 cm^2/g (Olivieri et al., 2024) to 136.3780 cm^2/g (Jamal AbuAlRoos et al., 2020 and Azman et al., 2023), compared to lead's MAC of 111.1520 cm^2/g. At moderate energies (100–1000 keV), tungsten-based material's MAC values are still higher, with a 100 keV value ranging from 2.5364 cm^2/g (Olivieri et al., 2024) to 4.3836 cm^2/g (Jamal AbuAlRoos et al., 2020 and Azman et al., 2023), compared to lead's 5.5496 cm^2/g. At high energies (1000 keV and above), tungsten's MAC converges with that of lead, with a 1000 keV value from 0.0654 cm^2/g (Lee et al., 2021) to 0.0667 cm^2/g (Das et al., 2023), while lead's is 0.0708 cm^2/g. Overall, tungsten-based materials offer superior attenuation at lower energies and comparable performance at higher energies.

Table 4. Mass attenuation coefficients (cm^2/g) and lead equivalent for tungsten-based materials at various energies

Energy (MeV)	AbuAlRoos et al., 2020	Azman et al., 2023	Pb Eq.	Lee et al., 2021	Pb Eq.	Das et al., 2023	Pb Eq.	Olivieri et al., 2024	Pb Eq.
0.015	136.3780	136.3780	1.2270	126.1490	1.1349	97.0939	0.8735	77.2264	0.6948
0.02	64.9188	64.9188	0.7541	59.9718	0.6967	46.2325	0.5371	36.7799	0.4273
0.03	22.4349	22.4349	0.7394	20.6911	0.6819	16.0079	0.5276	12.7550	0.4204
0.04	10.4978	10.4978	0.7315	9.6745	0.6741	7.5176	0.5238	6.0080	0.4187
0.05	5.8199	5.8199	0.7267	5.3634	0.6697	4.1901	0.5232	3.3637	0.4200
0.06	3.5971	3.5971	0.7225	3.3171	0.6662	2.6084	0.5239	2.1064	0.4231
0.08	7.7232	7.7232	3.2785	6.9941	2.9690	5.5312	2.3480	4.4201	1.8763
0.1	4.3836	4.3836	0.7899	3.9742	0.7161	3.1582	0.5691	2.5364	0.4570
0.15	1.5649	1.5649	0.7768	1.4258	0.7077	1.1528	0.5722	0.9426	0.4679
0.2	0.7777	0.7777	0.7773	0.7136	0.7133	0.5904	0.5902	0.4943	0.4940
0.3	0.3210	0.3210	0.7965	0.2998	0.7438	0.2613	0.6483	0.2298	0.5702
0.4	0.1911	0.1911	0.8236	0.1814	0.7819	0.1655	0.7136	0.1515	0.6531
0.5	0.1371	0.1371	0.8508	0.1319	0.8184	0.1247	0.7734	0.1173	0.7279
0.6	0.1088	0.1088	0.8723	0.1057	0.8478	0.1025	0.8219	0.0983	0.7887
0.8	0.0803	0.0803	0.9085	0.0791	0.8948	0.0792	0.8961	0.0778	0.8803
1	0.0659	0.0659	0.9314	0.0654	0.9246	0.0667	0.9431	0.0664	0.9383
1.5	0.0499	0.0499	0.9588	0.0499	0.9585	0.0516	0.9926	0.0519	0.9978
2	0.0442	0.0442	0.9630	0.0441	0.9604	0.0453	0.9867	0.0453	0.9874
3	0.0406	0.0406	0.9615	0.0401	0.9498	0.0400	0.9467	0.0393	0.9296
4	0.0402	0.0402	0.9592	0.0393	0.9389	0.0380	0.9085	0.0366	0.8749
5	0.0408	0.0408	0.9565	0.0396	0.9296	0.0374	0.8774	0.0354	0.8309
6	0.0418	0.0418	0.9540	0.0404	0.9219	0.0374	0.8530	0.0349	0.7965
8	0.0444	0.0444	0.9502	0.0425	0.9110	0.0382	0.8183	0.0349	0.7477
10	0.0471	0.0471	0.9474	0.0449	0.9034	0.0395	0.7953	0.0355	0.7154
15	0.0533	0.0533	0.9431	0.0504	0.8924	0.0431	0.7626	0.0379	0.6698

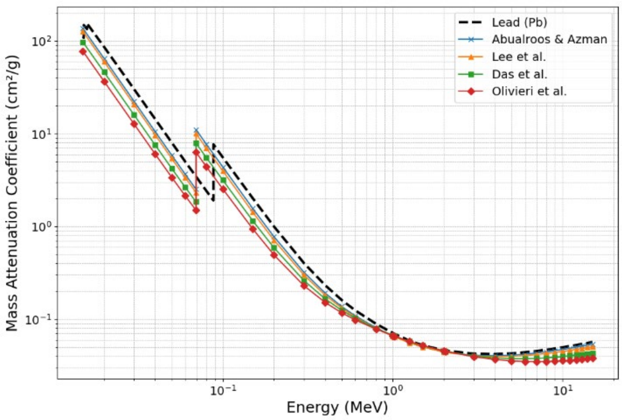

Figure 2. Mass attenuation coefficient values of various tungsten-based materials compared with lead

3.3. Barium (Ba)

Barium is the heaviest of the stable alkaline earth metals, with an atomic weight of 137.3, density of 3.62 g/cm3, and atomic number of 56. A soft metal that is silver-white and melts at 725°C is the free element. Barium volatiles, particularly halide salts, give the Bunsen flame a light green tint [77]. Barium as metal is generally non-toxic to humans and functions as a bone opacifier in the human body [78]. Barium oxide opens up new possibilities for environment friendly radiation shielding materials [79]. Due to its high atomic number and good attenuation coefficient, barium-based glasses have a very promising gamma radiation attenuation coefficient [30]. Due to its high density and atomic number, barium is a substance that is very good at absorbing ionizing radiation.

Barium oxide (BaO), for instance, can improve glass systems' capacity to guard against gamma radiation. strong atomic number, strong electrical resistance, high refraction, low coefficient of thermal expansion, low dispersion, and comparatively low melting point are only a few of barium's advantageous characteristics. Due to barium's high density and heavy-metal characteristics, adding more of it to materials enhances their shielding capabilities even further. Barium metal (99.2 + %) costs roughly \$3 per gram. Sen Baykal et al. designed and synthesized a lead-free, high-density borosilicate glass sample, BSBaZn, for potential use in radiation shielding applications in medical and industrial settings [80].

The glass composition is given by $7B_2O_3$-$50SiO_2$-38ZnO-5BaO. Structural and optical analyses, including FTIR spectroscopy, revealed four fundamental regions of interest in the glass, and it showed a transmittance rate of 80% in the 350–1100 nm wavelength range. Gamma-ray attenuation properties were assessed using a high-purity Germanium (HPGe) detector and a 133Ba radioisotope. The study employed the MCNPX Monte Carlo code to calculate gamma-ray transmission factors (TF) [56]. The results demonstrated that BSBaZn exhibits promising structural, optical, and gamma-ray shielding characteristics. Its high transparency and density make it a strong candidate for radiation protection in medical and industrial facilities where both source and patient monitoring are crucial [80].

Moradi et al. investigated barium tantalate (Ba5Ta4O15) as a lead-free alternative for x-ray shielding in interventional radiology [81]. Traditional lead-based materials, while effective, pose challenges due to their weight and toxicity. The study employed Geant4 Monte Carlo simulations to explore various barium tantalate formulations doped with rare earth elements. Results indicated that barium tantalate doped with 15% Erbium or 10% Samarium by weight offers effective x-ray shielding with over 30% weight reduction compared to lead-based materials. These findings suggest that barium tantalate could serve as a viable, lighter, and safer option for radiation shielding in medical settings [81].

Souza et al. introduced a novel, cost-effective lead-free elastomeric material for radiation shielding, designed to enhance user ergonomics while preventing exposure to harmful levels of ionizing radiation [82]. The material comprises a blend of 1 BaSO4 (barium sulfate) with 0.9 Si (silicon), 1.8 C (carbon), 5.4 H (hydrogen), and 0.9 O (oxygen), combined with addition-cure liquid silicone rubber. X-ray transmission measurements were performed for various thicknesses of this material and the results were compared with Monte Carlo simulations to ensure its effectiveness. The findings confirm that this material meets the requirements for use in radiation protection garments, offering a lighter and more ergonomic alternative to conventional lead-based shields [82].

Hannachi et al. explored a new ceramic-based material for γ-radiation shielding, specifically focusing on barium tungstate (BaWO4) doped with holmium oxide (Ho2O3) in varying amounts [83]. Monte Carlo simulations were employed to assess radiation attenuation. The radiation shielding coefficients decreased with higher Ho2O3 content. Specifically, the linear attenuation coefficient decreased by 13% from 0.386 cm^{-1} to 0.338 cm^{-1} at 0.662 MeV with an increase in Ho2O3 from 0% to 75%. Concurrently, the lead equivalent thickness increased from 3.22 cm to 3.67 cm. The optimal material identified in this study for γ-radiation shielding is a composite with 75% BaWO4 and 25% Ho2O3, as it provides a balance between shielding effectiveness and material composition [83].

Mass attenuation coefficient (MAC) values of the barium-based materials studied by the abovementioned groups are provided in Table 5 for various photon energies. These values were calculated for the composition of materials using the web database Epixs. Additionally, the MAC values are illustrated in Figure 3 as a function of energy, alongside those for lead.

As it can be seen from Figure 3, barium-based materials generally show lower MAC values than lead but are comparable at higher photon energies. At 15 keV, MAC values for the materials range from 5.4464 cm^2/g (Souza et al., 2023) to 89.9327 cm^2/g (Hannachi et al., 2023), which are lower than that of lead (111.1520 cm^2/g). At moderate energies (100–1000 keV), MAC values of the materials are significantly lower. For example, MAC values for 100 keV photon energy are ranging from 0.3535 cm^2/g (Souza et al., 2023) to 2.9686 cm^2/g (Hannachi et al., 2023), all are lower compared to lead's 5.5496 cm^2/g value. For higher photon energies (1000 keV and above), the MAC values for barium converge with those of lead. At 1000 keV energy, lead has 0.0708 cm^2/g MAC value, and materials have the values in a range between 0.0619 cm^2/g (Sen Baykal et al., 2023) and 0.0970 cm^2/g (Souza et al., 2023). Overall, it can be said that barium-based materials are less effective than lead at low and moderate photon energies, where attenuation is reduced. However, at higher energies their performance becomes comparable, making them a viable, safer, and more environmentally friendly alternative in specific high-energy applications across diverse medical imaging and therapy scenarios.

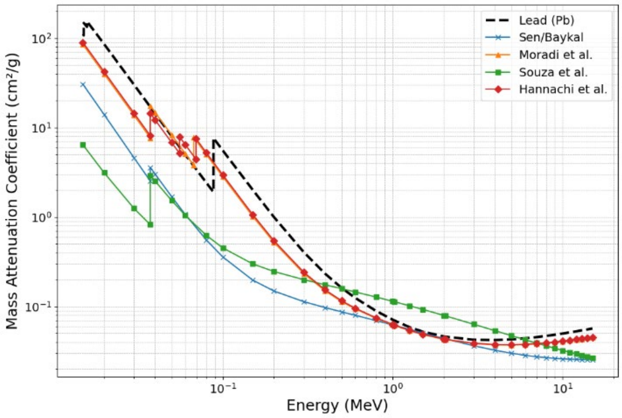

Figure 3. Mass attenuation coefficient values of various barium-based materials compared with lead

4. Other Emerging Materials

4.1. Tin (Sn)

Tin, which is not an essential metal, is a silvery, soft and pliable metal which resists corrosion and is widely used in industry and occurs in both inorganic and organic forms in nature. It has more commercially used organometallic derivatives than any other element, leading to a significant increase in global production of organotin compounds over the past decades. Due to their extensive industrial applications, substantial quantities of organotins have entered various ecosystems [84].

Tin (Sn) has an atomic weight of 118.69, an atomic number of 50, a density ranging from 5.8 to 7.3 (white tin), a melting point of 231.9°C, and a boiling point of 2602°C. Tin has three allotropic forms: white metallic, tetragonal (tin white), and white rhombic (tin brittle). When cooled below 13.2°C, it converts to gray tin or α-tin cubic [85]. Tin can be converted by chemical and biological reactions in the environment to form more toxic organotin compounds. Commercial tin has ranged in price over the last 25 years from 50¢/lb ($1.10/kg) to over $6/kg. Nowadays, a kilogram of pure tin costs roughly $260 [86].

Bjarnason et al. evaluated the absorption capability and weight of various lead-alternative radiation-shielding materials, focusing on tin, antimony, bismuth, and tungsten [87]. Factors such as toxicity, atomic number, density, K-edge absorption energy, and availability were considered. The attenuation coefficients of these elements were calculated using the XCOM software package [57], and the metals were mixed with polymers at mass ratios of 50%, 70%, 80%, and 85%. The study concluded that all new shielding materials tested are suitable for diagnostic X-ray applications. When compared to commercial lead garments, the 85% metal-polymer samples were lighter than a 0.5-mm lead garment and offered superior radiation protection. This suggests significant potential for these materials in commercial applications [87]. Bakhshandeh et al. explored the potential of a composite shield made from tin and tungsten as an alternative to traditional lead shields used in nuclear medicine [88]. Lead aprons, while effective, are criticized for their weight and toxicity. The study focused on evaluating the biological protection offered by the tin-tungsten composite compared to lead shields. Blood samples from non-radiation operatives were exposed to gamma radiation from technetium, and DNA damage was assessed. The composite shield demonstrated a density about one-tenth that of lead, at 1.23 g/cm³. Results indicated that DNA damage was lower with the lead-free shield compared to lead shields, with time being a significant factor in DNA damage, while the type of shield and distance did not show a significant effect. The study highlights the potential of tin-tungsten composites as alternative for reducing radiation-induced DNA damage, addressing the drawbacks of lead-based shielding [88].

Alım et al. investigated the potential of various alloys as replacements for lead and its derivatives in radiation shielding applications [89]. The study aimed to identify an optimal shielding material by evaluating the radiation-shielding characteristics of five different alloys: Tin-Silver, Manganin-R, Hastelloy-B, Hastelloy-X, and Dilver-P. Key photon interaction parameters were determined for these alloys across an energy range of 30 to 1333 keV using narrow-beam transmission geometry and experimental measurements with two detectors (Si(Li) and NaI(Tl)). The results were compared with theoretical calculations from Phy-X/PSD software. Finally, while Manganin-R alloy stands out as the superior shielding material for photon energies due to its high density, melting point, tensile strength, modulus of elasticity, and specific heat, the Tin-Silver alloy excels in aspects like attenuation coefficients [89].

Table 5. Mass attenuation coefficients (cm^2/g) and lead equivalent for barium-based materials at various energies

Energy (MeV)	Sen Baykal et al., 2023	Pb Eq.	Moradi et al., 2024	Pb Eq.	Souza et al., 2023	Pb Eq.	Hannachi et al., 2023	Pb Eq.
0.015	30.7976	0.2771	85.2541	0.7670	5.4464	0.0490	89.9327	0.8091
0.02	14.0786	0.1635	40.1536	0.4665	2.6018	0.0302	42.4186	0.4928
0.03	4.6220	0.1523	13.7212	0.4522	1.0176	0.0335	14.5221	0.4786
0.04	3.0146	0.2101	14.7046	1.0247	1.7718	0.1235	12.1147	0.8442
0.05	1.6941	0.2115	8.2566	1.0309	1.0996	0.1373	6.7796	0.8465
0.06	1.0753	0.2160	5.1129	1.0269	0.7670	0.1540	6.4625	1.2980
0.08	0.5561	0.2361	5.0138	2.1284	0.4734	0.2010	5.2568	2.2315
0.1	0.3584	0.0646	2.8285	0.5097	0.3535	0.0637	2.9686	0.5349
0.15	0.1971	0.0979	1.0200	0.5063	0.2447	0.1214	1.0696	0.5310
0.2	0.1487	0.1487	0.5212	0.5210	0.2049	0.2048	0.5450	0.5447
0.3	0.1129	0.2802	0.2327	0.5772	0.1681	0.4172	0.2410	0.5980
0.4	0.0969	0.4176	0.1490	0.6423	0.1480	0.6378	0.1532	0.6604
0.5	0.0868	0.5387	0.1132	0.7022	0.1341	0.8319	0.1158	0.7183
0.6	0.0795	0.6380	0.0938	0.7520	0.1236	0.9909	0.0955	0.7662
0.8	0.0692	0.7830	0.0732	0.8282	0.1081	1.2235	0.0741	0.8388
1	0.0619	0.8753	0.0620	0.8768	0.0970	1.3712	0.0626	0.8854
1.5	0.0504	0.9678	0.0484	0.9296	0.0788	1.5147	0.0487	0.9362
2	0.0436	0.9501	0.0427	0.9303	0.0675	1.4701	0.0430	0.9367
3	0.0362	0.8568	0.0383	0.9073	0.0539	1.2764	0.0386	0.9138
4	0.0322	0.7690	0.0370	0.8843	0.0458	1.0947	0.0373	0.8910
5	0.0298	0.6995	0.0369	0.8656	0.0405	0.9499	0.0372	0.8725
6	0.0283	0.6457	0.0373	0.8507	0.0367	0.8370	0.0376	0.8576
8	0.0266	0.5700	0.0387	0.8297	0.0316	0.6773	0.0391	0.8367
10	0.0258	0.5200	0.0405	0.8154	0.0284	0.5722	0.0409	0.8226
15	0.0253	0.4483	0.0449	0.7949	0.0240	0.4247	0.0453	0.8021

4.2. Cadmium (Cd)

Cadmium (Cd) with atomic number 48 and atomic weight 112.41. It belongs to group XII of the periodic table. Its soft, silvery-white metal, with a density of 8.65 g/cm³ and melting point of 321°C. Cadmium is soft, malleable, and ductile. It is resistant to corrosion, used as a protective plate, water-insoluble, and non-flammable, although it burns in air to form cadmium oxide. Cadmium, is a non-essential transition metal that can pose health risks to humans and animals due to its lack of a physiological function [90, 91].

El-Khatib et al. investigated HDPE composites with micro-sized and nano-sized cadmium oxide (CdO) particles for gamma radiation shielding [92]. The study found that nano-CdO/HDPE composites performed better than micro-CdO/HDPE, especially at low gamma-ray energies. The best performance was achieved with a composite of 40 wt% nano-CdO and 60 wt% HDPE, which showed a decent improvement in shielding at 59.53 keV due to the higher interaction probability between gamma-rays and nano-sized particles. From this study, it can be concluded that nano-CdO exhibits strong performance as a radiation shielding material [92].

4.3. Gadolinium (Gd)

Gadolinite is a soft, silvery-white rare-earth metal named after the Finnish chemist Gadolin. With an atomic number of 64 and an atomic weight of 157.25, gadolinium has a melting point of 1313 °C, a boiling point of 3273 °C, and density approximately 7.90 g/cm³ [93]. Gadolinium oxide, also known as gadolinia, is named after gadolinite, the mineral from which it was initially derived. Gadolinium is also present in other minerals such as monazite and bastnasite, which hold significant commercial value [48, 94].

Ogul et al. used 3D printing to create poly lactic acid (PLA) samples with 10% and 20% gadolinium oxide nanoparticles to evaluate their radiation shielding potential [95]. The optimal composition of the P-PLA-Gd20 sample was C 40.0009, H 4.4757, O 38.1767, and Gd 17.3467. This sample emerged as the best material, demonstrating excellent gamma-ray attenuation comparable to lead and achieving 100% thermal neutron shielding with a 10 mm thickness. This makes it a promising alternative to traditional lead aprons for both X-ray and neutron shielding [95].

4.4. Antimony (Sb)

Antimony is a silvery white metal with atomic number 51, and atomic mass 122. Antimony name is of Greek origin, “anti” plus “monos,” translating to “a metal not found alone”. This is accurate as native antimony metal is rarely found, it is usually discovered as a sulfide mineral, the most important being stibnite, Sb_2S_3. Antimony has a fairly low melting point for a metal, 630.6°C, is very brittle and a poor conductor of heat and electricity [96-98]. Antimony is typically used in combination with other materials for radiation shielding, particularly in alloys or composites, to enhance their protective properties against X-rays and gamma radiation. It is rarely used as a standalone shielding pmaterial [99, 100].

Özkalaycı et al. aimed to fabricate and investigate the gamma photon shielding efficiency of antimony (Sb) doped polymer resin composites [101]. They used orthophthalic unsaturated polyester resin ($C_{16}O_7H_{14}$) as the matrix and antimony powder as the filler. Sb particles were added to the composites in concentrations ranging from 5 to 20 wt%. Different isotopes were used to test gamma radiation shielding properties across energy levels from 59.5 to 1408.0 keV. To assess gamma-ray attenuation, the mass attenuation coefficient (MAC) was calculated, along with another key. Özkalaycı et al. found that a 20% antimony, 80% polyester resin composite provided the best gamma shielding among the tested Sb-doped polymers, showing superior attenuation performance [101].

4.5. Molybdenum (Mo)

Molybdenum, a trace element essential for microorganisms, plants, and animals, was discovered in 1778 by Karl Scheele, a Swedish scientist. It was originally thought to be lead, but its name, molybdos, comes from the Greek and means "lead-like." While molybdenum trioxide is a white powder that changes to a yellow substance when heated, molybdenum is a silver-white metal that can also be found as a black or dark-gray powder. The powdered form of molybdenite, also known as molybdenum disulfide, is gray and shiny. This metal has a melting temperature of 2610°C and a boiling point of 5560°C. Its atomic weight is 95.94 and its atomic number is 42 with density of 10.28 g/cm^3. Because it may give other materials hardness, weldability, and corrosion resistance, molybdenum is valued [102 - 105].

Al-Mugren et al. investigated HDPE composites doped with tungsten carbide, molybdenum carbide, and silicon carbide for kilovoltage radiation shielding. The produced shielding materials, composed of 85% HDPE and 15% MoC, were cut into disks, which were found to be lighter than lead (Pb). Findings suggest that HDPE composites doped with 15% MoC present the most promising configuration for low-energy X-ray shielding (30–50 keV) [106]. MACs and Pb-equivalents for tin, cadmium, gadolinium, antimony, and molybdenum are summarized in Table 6.

5. Performance Comparison and Discussion

5.1. Comparative MAC values

Mass attenuation coefficient (MAC) values of the investigated lead-free materials, namely bismuth, tungsten, barium, tin, cadmium, gadolinium, antimony and molybdenum, are presented in Tables 2–5 and Figures 1–4, with lead included as the reference material. At low photon energies in the range of 15–60 keV, where the photoelectric effect is the predominant interaction mechanism, materials with higher atomic numbers and densities demonstrate superior attenuation efficiency. Lead, with an atomic number of 82 and a density of 11.34 g/cm^3, consistently records the highest MAC values, reaching 111.1520 cm²/g at 15 keV. Tungsten, with a slightly lower atomic number but a significantly higher density of 19.3 g/cm³, achieves comparable or in some cases higher MAC values in this low-energy range, particularly in high-purity carbide forms.

Bismuth-based materials, benefitting from an atomic number of 83 and a density close to 9.8 g/cm³, also show strong attenuation performance, with several dense bismuth oxide and glass composites approaching or exceeding 100 cm²/g at 15 keV, highlighting their effectiveness for specialized shielding, diagnostic radiology, and potential advanced therapeutic applications in modern medical environments.

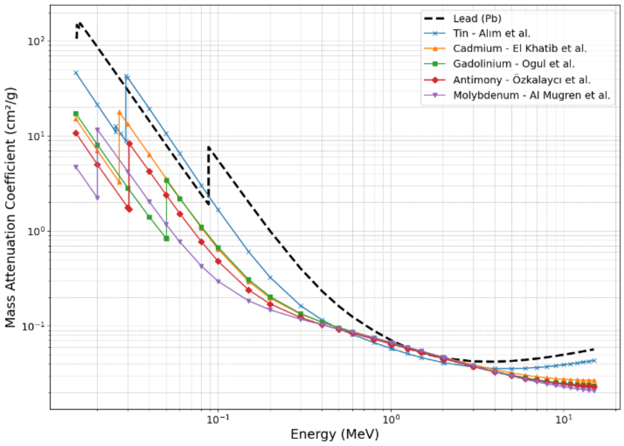

Figure 4. Mass attenuation coefficient values of various tin-, cadmium-, gadolinium-, antimony-, and molybdenum-based materials compared with lead

In contrast, barium-based materials, despite their usefulness in certain composite formulations, generally display lower MAC values unless present in high-density oxide or tungstate forms. Lower atomic number materials such as tin, cadmium, gadolinium, antimony and molybdenum exhibit noticeably reduced performance in this energy range; for instance, tin achieves 46.3733 cm²/g, gadolinium 17.2580 cm²/g and cadmium 15.1459 cm²/g, reflecting the strong dependence of photoelectric absorption probability on the cube of the atomic number. In the moderate photon energy range between 100 and 1000 keV, Compton scattering becomes the dominant interaction mechanism. In this regime, attenuation is influenced more by electron density than by atomic number alone, leading to a narrowing of the performance gap between lead and some of the high-density alternatives. Tungsten-based composites frequently reach MAC values close to those of lead, with high-performance formulations recording up to 4.38 cm²/g at 100 keV compared to lead's 5.5496 cm²/g. Bismuth-based glasses and polymer composites also perform competitively, with values around 4.6 cm²/g at the same energy. Barium-based systems, even when optimized, generally remain below 3.0 cm²/g at 100 keV, while among the lower atomic number group, molybdenum and tin perform better than cadmium, gadolinium and antimony due to their higher densities and more favorable electron densities. These observations indicate that in the Compton scattering–dominated energy range, high-density lead-free alternatives can provide attenuation performance that is suitable for many medical and industrial applications, even if they do not exactly match lead.

At high photon energies above 1000 keV, the influence of atomic number on attenuation efficiency decreases significantly as pair production and other high-energy processes become more relevant. Under these conditions, the MAC values of all investigated materials converge. At 1000 keV, lead's MAC value of 0.0708 cm²/g is essentially identical to that of molybdenum (0.0705 cm²/g) and only slightly higher than those of tungsten, bismuth, cadmium, gadolinium and certain high-density barium composites. This convergence confirms that at high energies, a variety of lead-free materials can provide comparable shielding performance, allowing the selection of materials to be guided by other considerations such as toxicity, environmental impact, cost, ease of fabrication and mechanical properties.

In summary, lead remains the most effective shielding material at low photon energies due to the strong atomic number dependence of the photoelectric effect, while tungsten and bismuth offer the closest overall performance across the full energy spectrum. Barium is more competitive at higher energies or when incorporated into optimized composite formulations, and lower atomic number materials, although less effective at low energies, become comparable to lead in the high-energy range.

These findings highlight the importance of matching the choice of shielding material to the photon energy range of interest, while also taking into account practical factors such as weight reduction, user comfort, cost-effectiveness and environmental sustainability in the development of next-generation radiation shielding solutions.

Table 6. Mass attenuation coefficients (cm^2/g) and lead equivalent for Tin, Cadmium, Gadolinium, Antimony and Molybdenum based materials at various energies

Energy (MeV)	Tin		Cadmium		Gadolinium		Antimony		Molybdenum	
	Alım, 2020	Pb Eq.	El-Khatib et al., 2019	Pb Eq.	Ogul et al., 2024	Pb Eq.	Özkalaycı et al., 2022	Pb Eq.	Al-mugren et al., 2024	Pb Eq.
0.015	46.3733	0.4172	15.1459	0.1363	17.2580	0.1553	10.7647	0.0968	4.4297	0.0399
0.02	21.2498	0.2469	6.9845	0.0811	8.1018	0.0941	4.9900	0.0580	2.0575	0.0239
0.03	40.7164	1.3419	13.3942	0.4414	2.8296	0.0933	1.7170	0.0566	3.9865	0.1314
0.04	19.3301	1.3470	6.3846	0.4449	1.3834	0.0964	4.2385	0.2954	1.9248	0.1341
0.05	10.6820	1.3338	3.5685	0.4456	0.8064	0.1007	2.4067	0.3005	1.1207	0.1399
0.06	6.5519	1.3159	2.2257	0.4470	2.1988	0.4416	1.5291	0.3071	0.7421	0.1490
0.08	3.0234	1.2834	1.0840	0.4602	1.1119	0.4720	0.7729	0.3281	0.4201	0.1783
0.1	1.6744	0.3017	0.6464	0.1165	0.6742	0.1215	0.4798	0.0864	0.2952	0.0532
0.15	0.6088	0.3022	0.2952	0.1465	0.3092	0.1535	0.2403	0.1193	0.1888	0.0937
0.2	0.3257	0.3255	0.1968	0.1967	0.2036	0.2035	0.1705	0.1705	0.1535	0.1535
0.3	0.1636	0.4059	0.1333	0.3308	0.1348	0.3344	0.1226	0.3042	0.1236	0.3065
0.4	0.1154	0.4974	0.1096	0.4724	0.1095	0.4718	0.1031	0.4445	0.1081	0.4660
0.5	0.0936	0.5807	0.0963	0.5977	0.0956	0.5934	0.0916	0.5685	0.0977	0.6062
0.6	0.0810	0.6497	0.0874	0.7007	0.0864	0.6930	0.0836	0.6702	0.0899	0.7213
0.8	0.0665	0.7529	0.0753	0.8517	0.0742	0.8392	0.0724	0.8191	0.0786	0.8894
1	0.0579	0.8187	0.0671	0.9477	0.0660	0.9321	0.0647	0.9138	0.0705	0.9963
1.5	0.0463	0.8906	0.0543	1.0438	0.0533	1.0240	0.0524	1.0077	0.0573	1.1011
2	0.0411	0.8946	0.0470	1.0238	0.0460	1.0012	0.0453	0.9855	0.0493	1.0726
3	0.0368	0.8722	0.0389	0.9221	0.0377	0.8931	0.0371	0.8784	0.0398	0.9426
4	0.0356	0.8493	0.0346	0.8260	0.0331	0.7915	0.0326	0.7777	0.0344	0.8205
5	0.0354	0.8311	0.0320	0.7496	0.0303	0.7105	0.0297	0.6975	0.0308	0.7233
6	0.0358	0.8164	0.0302	0.6899	0.0284	0.6475	0.0278	0.6351	0.0284	0.6477
8	0.0372	0.7966	0.0283	0.6060	0.0261	0.5585	0.0255	0.5471	0.0253	0.5409
10	0.0389	0.7834	0.0273	0.5507	0.0248	0.4998	0.0243	0.4891	0.0234	0.4706
15	0.0431	0.7625	0.0267	0.4721	0.0236	0.4172	0.0230	0.4071	0.0210	0.3714

6. Conclusion

In conclusion, this review highlights the critical need for alternatives to lead in radiation shielding, given its disadvantages, particularly in medical applications. While lead remains highly effective in attenuating radiation, its toxicity causes significant health risks to both patients and medical staff. Furthermore, environmental hazards associated with the disposal and potential contamination of lead compounds emphasize the urgency for safer, more sustainable options. The alternative materials examined in this review—Bismuth, Tungsten, Barium, Tin, Cadmium, Gadolinium, Antimony, and Molybdenum—demonstrate promising potential to address these challenges. Of these, Tungsten and Bismuth stand out because they are non-toxic, safe for the environment, and have a large amount of research and literature proving their effectiveness.

These materials not only reduce the health risks associated with lead but also align with modern sustainability goals by decreasing it's negative impacts. Although they come at a higher cost, their superior performance in radiation shielding, coupled with their safety profile, make them attractive candidates for further development. The shift toward these alternatives could greatly improve the safety standards of healthcare practices by eliminating the harmful side effects of lead, such as chronic toxicity and contamination risks. As ongoing research and technological advancements continue to enhance the performance and cost-efficiency of these materials, they hold the potential to revolutionize the future of medical radiation shielding. This transformation would not only ensure better protection for medical professionals and patients but also contribute to a significant reduction in the environmental effects of radiation shielding practices.

Finally, these emerging alternatives may play a pivotal role in shaping a safer and more sustainable approach to radiation protection in healthcare settings. Future research should prioritize the design and experimental validation of new composite materials that combine high atomic number (high-Z) elements with lightweight polymers or ceramics, aiming to achieve effective shielding with reduced mass. Comprehensive studies covering a wide photon energy range, along with cost and lifecycle analyses, will be important to assess their practical applicability.

Moreover, exploring additive manufacturing methods, such as 3D printing, could allow for the production of patient-specific or procedure-specific shielding devices, improving both radiation protection efficiency and user comfort in clinical environments.

Article Information Form

Authors' Contribution

Conceptualization, K.H.A. and H.A.; methodology, K.H.A.; literature collection and analysis, K.H.A. and H.A.; writing—original draft preparation, K.H.A.; writing—review and editing, K.H.A. and H.A.; supervision, H.A. All authors have read and agreed to the published version of the manuscript.

The Declaration of Conflict of Interest

No conflict of interest or common interest has been declared by authors.

Artificial Intelligence Statement

No artificial intelligence tools were used while writing this article.

Copyright Statement

References

[1] International Agency for Research on Cancer (IARC), IARC Monographs on the Evaluation of Carcinogenic Risks to Humans, Vol. 102: Non-Ionizing Radiation, Part 2: Radiofrequency Electromagnetic Fields. Lyon: IARC, 2013.

[2] Z. Huan, Y. Zheng, K. Wang, Z. Shen, W. Ni, J. Zua, Y. Shao, “Advancements in radiation resistance and reinforcement strategies of perovskite solar cells in space applications,” J. Mater. Chem. A, vol. 12, no. 4, pp. 1910–1922, 2024.

[3] H. Omer, “Radiobiological effects and medical applications of non-ionizing radiation,” Saudi Journal of Biological Sciences, vol. 28, no. 10, pp. 5585–5592, 2021.

[4] L. R. Dartnell, “Ionizing Radiation and Life,” Astrobiology, vol. 11, no. 6, pp. 551–582, 2011.

[5] G. Sgouros, “Alpha-particles for targeted therapy,” Advanced Drug Delivery Reviews, vol. 60, no. 12, pp. 1402–1406, 2008.

[6] B. Collum, “Radiation” in Nuclear Facilities, Elsevier, pp. 45–60, 2017.

[7] M. Bauckneht, C. Ciccarese, R. Laudicella, C. Mosillo, F. D’Amico, A. Anghelone, A. Strusi, V. Beccia, S. Bracarda, G. Fornarini, G. Tortora, R. Iacovelli, “Theranostics revolution in prostate cancer: Basics, clinical applications, open issues and future perspectives,” Cancer Treatment Reviews, vol. 124, p. 102698, 2024.

[8] U. Akar Tarim, “Assessment of the Usability of a Composite Containing Boron Carbide for Shielding the Gamma Rays,” Sakarya University Journal of Science, vol. 27, no. 1, pp. 159–167, 2023.

[9] S. Procz, C. Avila, J. Fey, G. Roque, M. Schuetz, E. Hamann, “X-ray and gamma imaging with Medipix and Timepix detectors in medical research,” Radiation Measurements, vol. 127, p. 106104, 2019.

[10] International Agency for Research on Cancer (IARC), Ed., A Review of Human Carcinogens (IARC Monographs on the Evaluation of Carcinogenic Risks to Humans, Vol. 100). Lyon: IARC, 2012.

[11] E. Mansouri, A. Mesbahi, R. Malekzadeh, A. Mansouri, “Shielding characteristics of nanocomposites for protection against X- and gamma rays in medical applications: effect of particle size, photon energy and nano-particle concentration,” Radiat Environ Biophys, vol. 59, no. 4, pp. 583–600, 2020.

[12] H. Kudo, Ed., Radiation Applications (An Advanced Course in Nuclear Engineering, Vol. 7). Singapore: Springer, 2018.

[13] J. G. Kiang, A. O. Olabisi, “Radiation: A poly-traumatic hit leading to multi-organ injury,” Cell Biosci, vol. 9, no. 1, p. 25, 2019.

[14] B. Barrett, M. Stiles, J. Patterson, “Radiation risks: Critical analysis and commentary,” Preventive Medicine, vol. 54, no. 3–4, pp. 280–282, 2012.

[15] D. İckecan, T. Nuredin, D. Erbahar, H. Gülbiçim, “Comparing the Shielding Features of Graphene and Impregnated Activated Carbon with Selected Traditional Shielding Materials for Gamma-Rays,” Sakarya University Journal of Science, vol. 27, no. 3, pp. 580–589, 2023.

[16] N. Voudoukis, S. Oikonomidis, “Inverse square law for light and radiation: A unifying educational approach,” EJERS, vol. 2, no. 11, p. 23, 2017.

[17] A. H. Patel, V. Patel, Y. Tang, S. Shah, G. Tang, M. J. Kern, “Implementing a ‘Lead [Apron]-Free’ Cardiac Catheterization: Current Status,” Curr Cardiol Rep, vol. 26, no. 9, pp. 1021–1029, 2024.

[18] J. H. Kim, “Three principles for radiation safety: Time, distance, and shielding,” Korean J Pain, vol. 31, no. 3, pp. 145–146, 2018.

[19] International Commission on Radiological Protection (ICRP), Recommendations of the International Commission on Radiological Protection: Adopted 1977 (Annals of the ICRP). 1977. [Online]. Available: https://books.google.com.tr/books?id=0gcaAQAAMAAJ.

[20] V. De Coninck, X. Mortiers, L. Hendrickx, S. De Wachter, O. Traxer, E. X. Keller, “Radiation exposure of patients during endourological procedures,” World J Urol, vol. 42, no. 1, p. 266, 2024.

[21] D. J. Greene, C. F. Tenggadjaja, R. J. Bowman, G. Agarwal, K. Y. Ebrahimi, D. D. Baldwin, “Comparison of a Reduced Radiation Fluoroscopy Protocol to Conventional Fluoroscopy During Uncomplicated Ureteroscopy,” Urology, vol. 78, no. 2, pp. 286–290, 2011.

[22] P. Limkitjaroenporn, W. Cheewasukhanont, S. Kothan, J. Kaewkhao, “Development of New High Transparency Pb-Free Radiation Shielding Glass,” Integrated Ferroelectrics, vol. 214, no. 1, pp. 181–204, 2021.

[23] C. V. More, Z. Alsayed, M. S. Badawi, A. A. Thabet, P. P. Pawar, “Polymeric composite materials for radiation shielding: A review,” Environ Chem Lett, vol. 19, no. 3, pp. 2057–2090, 2021.

[24] M. Balali-Mood, K. Naseri, Z. Tahergorabi, M. R. Khazdair, M. Sadeghi, “Toxic mechanisms of five heavy metals: Mercury, lead, chromium, cadmium, and arsenic,” Front. Pharmacol., vol. 12, 2021.

[25] P. B. Tchounwou, C. G. Yedjou, A. K. Patlolla, D. J. Sutton, “Heavy metals toxicity and the environment,” EXS, vol. 101, pp. 133–164, 2012.

[26] I. Erkoyuncu, F. Akman, H. Ogul, M. R. Kaçal, H. Polat, I. Demirkol, K. Dilsiz, B. Ertuğral, “A detailed investigation of gamma and neutron shielding capabilities of ternary composites doped with polyacrylonitrile and gadolinium (III) sulfate,” Applied Radiation and Isotopes, vol. 196, p. 110789, 2023.

[27] Canada Metal (Pacific) Ltd. 2016. A guide to the use of lead for radiation shielding [Online]. Available: https://www.canadametal.com/radiation-protection/.

[28] M. Donya, M. Radford, A. ElGuindy, D. Firmin, M. H. Yacoub, “Radiation in medicine: Origins, risks and aspirations,” Global Cardiology Science and Practice, vol. 2014, no. 4, p. 57, 2014.

[29] N. J. AbuAlRoos, N. A. Baharul Amin, R. Zainon, “Conventional and new lead-free radiation shielding materials for radiation protection in nuclear medicine: A review,” Radiation Physics and Chemistry, vol. 165, p. 108439, 2019.

[30] A. A. Oglat, S. M. Shalbi, “An Alternative Radiation Shielding Material Based on Barium-Sulphate (BaSO4)-Modified Fly Ash Geopolymers,” Gels, vol. 8, no. 4, p. 227, 2022.

[31] M. Almurayshid, Y. Alssalim, F. Aksouh, R. Almsalam, M. ALQahtani, M. I. Sayyed, F. Almasoud, “Development of New Lead-Free Composite Materials as Potential Radiation Shields,” Materials, vol. 14, no. 17, p. 4957, 2021.

[32] S. Muir, R. McLeod, R. Dove, “Light-weight lead aprons—light on weight, protection or labelling accuracy?” Australas. Phys. Eng. Sci. Med., vol. 28, no. 2, pp. 128–130, 2005.

[33] X.-L. Ni, J.-L. Li, J.-H. Lv, Z.-J. Liao, C. Yang, J. Zeng, Y.-J. Li, Y.-T. Li, Y.-L. Zhou, Q.-P. Zhang, “Intensely bonded high filling bismuth oxide with chloroprene rubber to achieve lead-free flexible materials for γ-rays shielding,” Radiation Effects and Defects in Solids, pp. 1–13, 2024.

[34] E. Kusiak, M. Zaborski, W. Baryń, “Lead-free elastomers composites as X-ray radiation-absorbing materials,” Przemysl Chemiczny, vol. 90, no. 5, pp. 874–877, 2011.

[35] P. Lim-aroon, E. Wimolmala, N. Sombatsompop, K. Saenboonruang, “Manufacturing process and properties of lead-free natural rubber sponge for use in X-ray and gamma ray shielding applications,” IOP Conf. Ser.: Mater. Sci. Eng., vol. 526, no. 1, p. 012015, 2019.

[36] S. M. J. Mortazavi, A. Zahiri, D. Shahbazi-Gahrouei, S. Sina, M. Haghani, “Designing a shield with lead-free polymer base with high radiation protection for X-ray photons in the range of diagnostic radiology using monte carlo simulation code MCNP5,” Journal of Isfahan Medical School, vol. 34, no. 385, pp. 637–641, 2016.

[37] K. Yue, W. Luo, X. Dong, C. Wang, G. Wu, M. Jiang, Y. Zha, “A new lead-free radiation shielding material for radiotherapy,” Radiation Protection Dosimetry, vol. 133, no. 4, pp. 256–260, 2009.

[38] V. P. Singh, N. M. Badiger, “An investigation on gamma and neutron shielding efficiency of lead-free compounds and alloys,” Indian Journal of Pure and Applied Physics, vol. 54, no. 7, pp. 443–448, 2016.

[39] O. Bawazeer, A. Fallatah, M. Alasmary, Y. Bokhary, A. Almerabi, S. Khan, N. Abuhadi, A. Alalawi, N. Asiri, S. Bawazir, S. Al-Qahtani, M. Algethami, M. Badawy, “Investigation of barium sulphate shielding during panoramic radiography,” Egypt J

Radiol Nucl Med, vol. 54, no. 1, p. 203, 2023.

[40] M. Ghasemi-Nejad, L. Gholamzadeh, R. Adeli, S. P. Shirmardi, “The effect of modified Tin oxide on X-ray attenuation: An experimental and theoretical study,” Nuclear Instruments and Methods in Physics Research Section B: Beam Interactions with Materials and Atoms, vol. 549, p. 165277, 2024.

[41] M. Ghasemi-Nejad, L. Gholamzadeh, R. Adeli, S. P. Shirmardi, “A comprehensive study of the antibacterial and shielding properties of micro and nano-EPVC lead-free shields,” Phys. Scr., vol. 97, no. 5, 2022.

[42] C. R. Blackwell, K. D. Amundson, “Cadmium free lead alloy for reusable radiotherapy shielding,” Medical Dosimetry, vol. 15, no. 3, pp. 127–129, 1990.

[43] D.-E. Kwon, D.-H. Han, K.-H. Jung, S.-J. Lee, J.-O. Kim, C.-H. Baek, “Performance and feasibility evaluation for radiation shielding of metal oxides: Monte Carlo simulation,” J. Korean Phys. Soc., vol. 82, no. 8, pp. 813–817, 2023.

[44] H. Schlattl, M. Zankl, H. Eder, C. Hoeschen, “Shielding properties of lead-free protective clothing and their impact on radiation doses,” Medical Physics, vol. 34, no. 11, pp. 4270–4280, 2007.

[45] M.-A. Shahbazi, L. Faghfouri, M. P. A. Ferreira, P. Figueiredo, H. Maleki, F. Sefat, J. Hirvonen, H. A. Santos, “The versatile biomedical applications of bismuth-based nanoparticles and composites: therapeutic, diagnostic, biosensing, and regenerative properties,” Chem. Soc. Rev., vol. 49, no. 4, pp. 1253–1321, 2020.

[46] Y. Xin, Z. Wang, C. Yao, H. Shen, Y. Miao, “Bismuth, a Previously Less-studied Element, Is Bursting into New Hotspots,” ChemistrySelect, vol. 7, no. 21, p. e202201220, 2022.

[47] H.-T. Sun, J. Zhou, J. Qiu, “Recent advances in bismuth activated photonic materials,” Progress in Materials Science, vol. 64, pp. 1–72, 2014.

[48] W. M. Haynes, D. R. Lide, T. J. Bruno, CRC Handbook of Chemistry and Physics, 2016–2017, 97th ed. Boca Raton, FL: CRC Press, 2016.

[49] F. Bakri, P. L. Gareso, D. Tahir, “Advancing radiation shielding: A review the role of Bismuth in X-ray protection,” Radiation Physics and Chemistry, vol. 217, p. 111510, 2024.

[50] G. Toshinsky, V. Petrochenko, “Modular Lead-Bismuth Fast Reactors in Nuclear Power,” Sustainability, vol. 4, no. 9, pp. 2293–2316, 2012.

[51] N. J. Abualroos, K. A. Yaacob, R. Zainon, “Radiation attenuation effectiveness of polymer-based radiation shielding materials for gamma radiation,” Radiation Physics and Chemistry, vol. 212, p. 111070, 2023.

[52] R. U. Ayres, L. W. Ayres, I. Råde, “Lead, Zinc and Other Byproduct Metals,” in The Life Cycle of Copper, Its Co-Products and Byproducts, R. U. Ayres, L. W. Ayres, and I. Råde, Eds., Dordrecht: Springer Netherlands, 2003, pp. 101–147.

[53] T. Ibn-Mohammed, I. M. Reaney, S. C. L. Koh, A. Acquaye, D. C. Sinclair, C. A. Randall, F. H. Abubakar, L. Smith, G. Schileo, L. Ozawa-Meida., “Life cycle assessment and environmental profile evaluation of lead-free piezoelectrics in comparison with lead zirconate titanate,” Journal of the European Ceramic Society, vol. 38, no. 15, pp. 4922–4938, 2018.

[54] A. T. Odularu, “Bismuth as Smart Material and Its Application in the Ninth Principle of Sustainable Chemistry,” Journal of Chemistry, vol. 2020, pp. 1–15, 2020.

[55] M. Karimi, K. Ghazikhanlou-sani, A. R. Mehdizadeh, H. Mostaghimi, “Lead-free transparent shields for diagnostic X-rays: Monte Carlo simulation and measurements,” Radiol Phys Technol, vol. 13, no. 3, pp. 276–287, 2020.

[56] L. S. Waters, G. W. McKinney, J. W. Durkee, M. L. Fensin, J. S. Hendricks, M. R. James, R. C. Johns, D. B. Pelowitz., “The MCNPX Monte Carlo Radiation Transport Code,” in AIP Conf. Proc., Batavia, IL, USA, 2007, pp. 81–90.

[57] S. M. Seltzer. (1987). XCOM: Photon Cross Sections Database (NIST Standard Reference Database 8) [Online]. Available: https://www.nist.gov/pml/xcom-photon-cross-sections-database .

[58] L. Yu, P. L. Yap, A. Santos, D. Tran, D. Losic, “Lightweight Bismuth Titanate (Bi 4 Ti 3 O 12) Nanoparticle-Epoxy Composite for Advanced Lead-Free X-ray Radiation Shielding,” ACS Appl. Nano Mater., vol. 4, no. 7, pp. 7471–7478, 2021.

[59] T. H. Khazaalah, I. S. Mustafa, H. Al-Ghamdi, A. A. Rahman, M. I. Sayyed, A. H. Almuqrin, M. H. M. Zaid, R. Hisam, M. F. I. A. Malik, N. S. Ezra, H. M. Shariff, “The Effect of WO3-Doped Soda Lime Silica SLS Waste Glass to Develop Lead-Free Glass as a Shielding Material against Radiation,” Sustainability, vol. 14, no. 4, p. 2413, 2022.

[60] W. Li, S. Chen, M. Peng, X. Zhou, X. Zhao, “Radiation shielding design and development of Bi/Ta/PU lead-free flexible textile composites,” J. Ind. Textiles, vol. 53, 2023.

[61] S. Jing, H. Liqin, L. Pengcheng, H. Tao, H. Lijuan, C. Mengyun, Z. Huaqing, Y. Shengpeng, S. Guangyao, D. Tongqiang, Y. Qi, W. Bin, C. Chaobin, F. Ling, Y. Qianfeng, W. Yican, FDS Team, “Monte Carlo Simulation Software SuperMC 2.3 for Fusion and Fission Applications,” in Proc. Reactor Physics Asia 2015 (RPHA15), Jeju, Korea, 2015.

[62] M. A. M. Uosif, S. A. M. Issa, A. Ene, A. M. A. Mostafa, A. Atta, E. F. El Agammy, H. M. H. Zakaly, “Lead-free ternary glass for radiation protection: Composition and performance evaluation for solar cell coverage,” Materials, vol. 16, no. 8, p. 3036, 2023.

[63] Y. Al-Hadeethi, M. I. Sayyed, A. Z. Barasheed, M. Ahmed, M. Elsafi, “Fabrication of lead-free borate glasses modified by bismuth oxide for gamma ray protection applications,” Materials, vol. 15, no. 3, p. 789, 2022.

[64] J.-H. Liu, Q.-P. Zhang, N. Sun, Y. Zhao, R. Shi, Y.-L. Zhou, J. Zheng, “Elevated gamma-rays shielding property in lead-free bismuth tungstate by nanofabricating structures,” Journal of Physics and Chemistry of Solids, vol. 112, pp. 185–189, 2018.

[65] S. K. Das, C. H. R. V. S. Nagesh, T. Sreenivas, T. Kundu, S. I. Angadi, “A treatise on occurrence, beneficiation and plant practices of tungsten-bearing ores,” Powder Technology, vol. 429, p. 118938, 2023.

[66] P. E. Leffler, G. Kazantzis, “Tungsten,” in Handbook on the Toxicology of Metals, G. F. Nordberg, B. A. Fowler, and M. Nordberg, Eds. Amsterdam: Elsevier, 2015, pp. 1297–1306.

[67] W. Cheewasukhanont, P. Limkitjaroenporn, M. I. Sayyed, S. Kothan, H. J. Kim, J. Kaewkhao, “High density of tungsten gadolinium borate glasses for radiation shielding material: Effect of WO3 concentration,” Radiation Physics and Chemistry, vol. 192, p. 109926, 2022.

[68] S. Kobayashi, N. Hosoda, R. Takashima, “Tungsten alloys as radiation protection materials,” Nuclear Instruments and Methods in Physics Research Section A: Accelerators, Spectrometers, Detectors and Associated Equipment, vol. 390, no. 3, pp. 426–430, 1997.

[69] J. Webb, S. Gollapudi, I. Charit, "An overview of creep in tungsten and its alloys," International Journal of Refractory Metals and Hard Materials, vol. 82, pp. 69–80, 2019.

[70] Y. Taki, K. Shinozaki, T. Honma, V. Dimitrov, T. Komatsu, "Electronic polarizability and interaction parameter of gadolinium tungsten borate glasses with high WO3 content," Journal of Solid State Chemistry, vol. 220, pp. 191–197, 2014.

[71] N. Jamal AbuAlRoos, M. N. Azman, N. A. Baharul Amin, R. Zainon, "Tungsten-based material as promising new lead-free gamma radiation shielding material in nuclear medicine," Physica Medica, vol. 78, pp. 48–57, 2020.

[72] M. N. Azman, N. J. Abualroos, K. A. Yaacob, R. Zainon, "Feasibility of nanomaterial tungsten carbide as lead-free nanomaterial-based radiation shielding," Radiation Physics and Chemistry, vol. 202, p. 110492, 2023.

[73] T. Lee, C. Yoon, S. Jo, N. Kim, "Performance estimation of lead-free dual-layered shielding in dismantling of steam generator: A Monte-Carlo simulation study," Applied Radiation and Isotopes, vol. 176, p. 109879, 2021.

[74] G. Battistoni, J. Bauer, T. T. Boehlen, F. Cerutti, M. P. W. Chin, R. Dos Santos Augusto, A. Ferrari, P. G. Ortega, W. Kozłowska, G. Magro, A. Mairani, K. Parodi, P. R. Sala, P. Schoofs, T. Tessonnier, V. Vlachoudis, "The FLUKA Code: An Accurate Simulation Tool for Particle Therapy," Front Oncol, vol. 6, p. 116, 2016.

[75] A. Das, A. Ray, T. Singh, "Tungsten-based polymer composite, a new lead-free material for efficient shielding of coupled neutron-gamma radiation fields: A FLUKA simulation study," Phys. Scr., vol. 98, no. 11, p. 115302, 2023.

[76] F. Olivieri, R. Avolio, G. Gentile, A. Mazzone, R. Rizzi, M. Nacucchi, R. Castaldo, M. E. Errico, C. Giannini, L. Ambrosio, M. Lavorgna, "High filler content acrylonitrile-butadiene-styrene composites containing tungsten and bismuth oxides for effective lead-free x-ray radiation shielding," Polymer Composites, vol. 45, no. 3, pp. 2101–2113, 2024.

[77] A. Oskarsson, "Chapter 4 – Barium," in Handbook on the Toxicology of Metals (Fifth Edition), G. F. Nordberg and M. Costa, Eds. Amsterdam: Academic Press, pp. 91–100, 2022.

[78] G. Kaur, S. G. Waldrop, V. Kumar, O. P. Pandey, N. Sriranganathan, "An Introduction and History of the Bioactive Glasses," in Biocompatible Glasses, J. Marchi, Ed., Advanced Structured Materials, vol. 53. Cham: Springer International Publishing, pp. 19–47, 2016.

[79] J. Singh, V. Kumar, Y. K. Vermani, M. S. Al-Buriahi, J. S. Alzahrani, T. Singh, "Fabrication and characterization of barium based bioactive glasses in terms of physical, structural, mechanical and radiation shielding properties," Ceramics International, vol. 47, no. 15, pp. 21730–21743, 2021.

[80] D. S. Baykal, G. Kilic, E. Ilik, E. Kavaz, G. ALMisned, R. B. Cakirli, H. O. Tekin, "Designing a Lead-free and high-density glass for radiation facilities: Synthesis, physical, optical, structural, and experimental gamma-ray transmission properties of newly designed barium-borosilicate glass sample," Journal of Alloys and Compounds, vol. 965, p. 171392, 2023.

[81] F. Moradi, M. Jalili, K. R. E. Saraee, M. R. Abdi, H. A. A. Rashid, "Radiation shielding assessment for interventional radiology personnel: Geant4 dosimetry of lead-free compositions," Biomed. Phys. Eng. Express, vol. 10, no. 2, p. 025029, 2024.

[82] E. G. Souza, K. Kruger, C. D. Nascimento, C. Aguzzoli, G. Hoff, A. C. B. K. Moraes, R. G. Lund, P. S. Nascente, C. E. Cuevas-Suárez, E. Piva, N. L. V. Carreno, "Development of lead-free radiation shielding material utilizing barium sulfate and magnesium oxide as fillers in addition cure liquid silicone rubber," Polymers, vol. 15, no. 22, p. 4382, 2023.

[83] E. Hannachi, Y. Slimani, M. I. Sayyed, K. G. Mahmoud, "Scheelite-type BaWO4 doped with Ho2O3 oxide as a promising lead-free shield for gamma rays: Structural, optical properties, and radiation attenuation efficiency," Materials Science in Semiconductor Processing, vol. 167, p. 107802, 2023.

[84] M. Hoch, "Organotin compounds in the environment—an overview," Applied Geochemistry, vol. 16, pp. 719–743, 2001.

[85] B. Cornelius, S. Treivish, Y. Rosenthal, M. Pecht, "The phenomenon of tin pest: A review," Microelectronics Reliability, vol. 79, pp. 175–192, 2017.

[86] G. Nordberg, Handbook on the toxicology of metals, 3rd ed. Amsterdam Boston: Academic Press, 2007.

[87] T. A. Bjarnason, "Letter to the editor: The absorption properties of lead-free garments for use in radiation protection," Radiation Protection Dosimetry, vol. 179, no. 3, pp. 253–253, 2018.

[88] M. Bakhshandeh, M. B. Ziarani, M. B. Farsani, E. Bakhshandeh, N. Shakeri, "Review and performance comparison of lead-free shields and lead shields, in terms of biological effects in nuclear medicine by the comet method," Koomesh, vol. 20, no. 4, pp. 792–799, 2018.

[89] B. Alım, "A comprehensive study on radiation shielding characteristics of Tin-Silver, Manganin-R, Hastelloy-B, Hastelloy-X and Dilver-P alloys," Appl. Phys. A, vol. 126, no. 4, p. 262, 2020.

[90] K. A. Isimekhai, "Environmental risk assessment for an informal E-Waste recycling site in Lagos State, Nigeria," Middlesex University, London, 2016.

[91] G. Genchi, M. S. Sinicropi, G. Lauria, A. Carocci, A. Catalano, "The Effects of Cadmium Toxicity," IJERPH, vol. 17, no. 11, p. 3782, 2020.

[92] A. M. el-Khatib, M. I. Abbas, M. Abd elzaher, M. S. Badawi, M. T. Alabsy, G. A. Alharshan, D. A. Aloraini "Gamma Attenuation Coefficients of Nano Cadmium Oxide/High density Polyethylene Composites," Sci Rep, vol. 9, no. 1, p. 16012, 2019.

[93] L. Obied, "Infrared Spectroscopy of Gadolinium," Brock University, 2013. [Online]. Available: http://hdl.handle.net/10464/4275

[94] L. Blomqvist, G. F. Nordberg, V. M. Nurchi, J. O. Aaseth, "Gadolinium in Medical Imaging—Usefulness, Toxic Reactions and Possible Countermeasures—A Review," Biomolecules, vol. 12, no. 6, p. 742, 2022.

[95] H. Ogul, B. Gultekin, H. Yildiz, H. Us, F. Bulut, "Novel 3D-Printed lead-free radiation protection apron in the medical X-ray and thermal neutron energy range," Radiation Physics and Chemistry, vol. 219, p. 111686, 2024.

[96] S. Sundar, J. Chakravarty, "Antimony Toxicity," IJERPH, vol. 7, no. 12, pp. 4267–4277, 2010.

[97] R. S. Multani, T. Feldmann, G. P. Demopoulos, "Antimony in the metallurgical industry: A review of its chemistry and environmental stabilization options," Hydrometallurgy, vol. 164, pp. 141–153, 2016.

[98] C. Reimann, J. Matschullat, M. Birke, R. Salminen, "Antimony in the environment: Lessons from geochemical mapping,"

Applied Geochemistry, vol. 25, no. 2, pp. 175–198, 2010.

[99] C. Zeng, Q. Kang, Z. Duan, B. Qin, X. Feng, H. Lu, Y. Lin, "Development of polymer composites in radiation shielding applications: A review," J Inorg Organomet Polym, vol. 33, no. 8, pp. 2191–2239, 2023, https://doi.org/10.1007/s10904-023-02725-6

[100] S. Wu, J. Bao, Y. Gao, W. Hu, Z. Lu, "Review on flexible radiation-protective clothing materials," J Mater Sci, vol. 59, no. 19, pp. 8109–8133, 2024.

[101] F. Özkalaycı, M. R. Kaçal, H. Polat, O. Agar, N. Almousa, F. Akman, "Lead-free Sb-based polymer composite for γ-ray shielding purposes," Radiochimica Acta, vol. 110, no. 5, pp. 393–402, 2022.

[102] J. A. Novotny, C. A. Peterson, "Molybdenum," Advances in Nutrition, vol. 9, no. 3, pp. 272–273, 2018.

[103] D. G. Barceloux, D. Barceloux, "Molybdenum," Journal of Toxicology: Clinical Toxicology, vol. 37, no. 2, pp. 231–237, 1999.

[104] J. M. Khurana, S. Chauhan, A. Agrawal, "Molybdenum in organic synthesis: A review," Organic Preparations and Procedures International, vol. 36, no. 3, pp. 201–276, 2004.

[105] J. A. Novotny, "Molybdenum nutriture in humans," J Evid Based Complementary Altern Med, vol. 16, no. 3, pp. 164–168, 2011.

[106] K. S. Al-mugren, L. Almalki, R. Alshehri, S. Alamri, M. Almurayshid, M. Alsuhybani, R. Alharbi, M. U. Khandaker, "Development of lead-free metal carbides and ceramic decorated HDPE composites for low energy X-ray shielding applications," Radiation Physics and Chemistry, vol. 220, p. 111688, 2024.